Virology 412 (2011) 36–45

Contents lists available at ScienceDirect

Virology

journal homepage: www.elsevier.com/locate/yviro

Pathogenicity of different PR8 influenza A virus variants in mice is determined by both viral and host factors

Paulina Blazejewska [a], Lukasz Koscinski [b], Nuno Viegas [a], Darisuren Anhlan [c], Stephan Ludwig [c], Klaus Schughart [a,*]

[a] Department of Infection Genetics, Helmholtz Centre for Infection Research and University of Veterinary Medicine Hannover, 38124 Braunschweig, Germany
[b] Laboratory of Structural Bioinformatics, Faculty of Biology, Adam Mickiewicz University, Umultowska 89, 61-614 Poznan, Poland
[c] Institute of Molecular Virology, Von Esmarch Str 56, 48149 Muenster, Germany

ARTICLE INFO

Article history:
Received 22 July 2010
Returned to author for revision
19 August 2010
Accepted 23 December 2010
Available online 22 January 2011

Keywords:
Mouse genetics
Influenza
PR8
H1N1
Inbred strains
Host response
Pathogenesis

ABSTRACT

Experimental mouse models were used to compare virulence and reproduction rate of three mouse-adapted variants of the PR8 influenza A virus strain. We observed large differences in pathogenicity in two mouse strains. The PR8M variant was lethal in DBA/2J mice but not in C57BL/6J mice, whereas PR8F and hvPR8 variants were lethal in both mouse strains. High lethality of PR8M in DBA/2J correlated with high viral load at early time points after infection and spread of the virus into alveolar regions. Also, higher viral loads and mortality in mice infected with PR8F resulted in a higher number of infiltrating leukocytes. 3D-protein structure predictions of the HA indicated amino acid sequence alterations which may render the HA cleavage site in PR8F more accessible to host proteases. Infection of C57BL/6J mice with a re-assorted PR8 virus revealed that the HA gene is the main determinant of virulence of the PR8F variant.

Introduction

The course and outcome of an influenza virus A infection is influenced by several viral and host factors. Virulence factors of the virus determine its host specificity but also the severity of disease (Ducatez et al., 2008; Jang et al., 2009; Krug, 2006; Rolling et al., 2009; Salomon and Webster, 2009; Scheiblauer et al., 1995; Song et al., 2009; Yen et al., 2009). Reports on host factors regulating viral propagation are manifold and include importins (Gabriel et al., 2008), kinases (Pleschka et al., 2001), caspases (e.g. (Wurzer et al., 2003) or effectors of the type I interferon response (Haller et al., 2009). Furthermore, other risk factors of the host like obesity or pregnancy became evident during the recent swine flu pandemics (Scriven et al., 2009; Yates et al., 2010). Furthermore, genetic factors in humans associated with a higher susceptibility to influenza infections and severe disease outcome have been suspected for the 1918 pandemics as well as the H5N1 human infections (Albright et al., 2008; Gottfredsson et al., 2008; Horby et al., 2010).

The main antigenic determinants of influenza A viruses are the haemagglutinin (HA) and the neuraminidase (NA) genes. Based on the antigenicity of these membrane-associated glycoproteins, sixteen HA (H1–H16) and nine NA (N1–N9) subtypes (Bouvier and Palese, 2008) have been described until now. Influenza A virus enters the host cells through binding of the HA protein to the N-acetylneuraminic (sialic) acids (alpha 2,3 or alpha 2,6) present on the cell surface. The binding to sialic acids occurs via the interaction of a depression at the distal surface of the globular head of the HA molecule (Weis et al., 1988). The influenza HA protein (HA0) is synthesized as an immature protein and is cleaved by host proteases into the two subunits HA1 and HA2. Cleavage is required for infectivity and is an important determinant for pathogenicity in human and avian hosts. The HA1 subunit represents the receptor binding domain, whereas the HA2 subunit contains the fusion peptide. Furthermore, influenza virus can adapt to new host species through the modification of the HA protein sequence, especially at the cleavage site (Couceiro et al., 1993; Matrosovich et al., 2004). In experimental systems, adaptation can be achieved via several passages in a new host which results in variations of the receptor-binding site in the HA (Grimm et al., 2007) as well as modifications of NA and polymerase genes. However, there are also examples of H5 and H7 virus subtypes isolated from birds (Belser et al., 2007; Gao

* Corresponding author. Inhoffenstr.7, D-38124 Braunschweig, Germany. Fax: +49 5312 6181 1199.
E-mail address: klaus.schughart@helmholtz-hzi.de (K. Schughart).

0042-6822/$ – see front matter © 2010 Elsevier Inc. All rights reserved.
doi:10.1016/j.virol.2010.12.047

et al., 1999) as well as the vH1N1/2009 which can replicate in mice without prior adaptation (Belser et al., 2010).

In this study, we used three different mouse-adapted variants of the influenza virus strain A/Puerto Rico/8/34. The PR8M and PR8F variants are closely related in sequence to the PR8 Mount Sinai strain (Schickli et al., 2001). These two variants were derived from the same ancestor but did acquire some additional changes when propagated in different laboratories (PR8M in Muenster and PR8F variant in Freiburg, see Materials and methods for details). The hvPR8 is a variant of the PR8 Cambridge strain and is more distantly related to the other two variants. It exhibits an extremely high replication rate in mice which is a decisive factor in the lethal outcome of infection (Grimm et al., 2007).

In mouse model systems, genetic factors, such as gene mutations (*e.g. Mx1*, *Stat1*, *Pkr*, *Infar1*, *Ncr1* — (Bergmann et al., 2000; Gazit et al., 2006; Haller et al., 1976; Koerner et al., 2007; Tumpey et al., 2007) as well as differences in the genetic background (Boon et al., 2009, 2010; Ding et al., 2008; Srivastava et al., 2009) have been clearly demonstrated to play an important role in host susceptibility or resistance to infection. Using the mouse-adapted PR8M (H1N1) variant and the strain A/Seal/Massachusetts/1/80 (H7N7; SC35M) we previously showed that DBA/2J mice are highly susceptible to both virus subtypes whereas C57BL/6J mice are resistant (Srivastava et al., 2009).

Here, we demonstrate that there are large differences in pathogenicity of the three mouse-adapted PR8 influenza A variants in two inbred mouse strains. While the PR8M variant is only lethal for DBA/2J mice, the PR8F and the hvPR8 variants were lethal for both, DBA/2J and C57BL/6J mouse strains. The high lethality of PR8F and hvPR8 correlated with high viral load. Also, PR8F infected C57BL/6J mice showed a higher number of infiltrating leukocytes in infected lungs compared to PR8M infected mice. Sequence comparisons and subsequent 3D-predictions of the HA variants from PR8M and PR8F indicated differences in the folding of the HA which may influence its interaction with cellular proteases and thus might contribute to the higher virulence of the PR8F variant. Infection of C57BL/6J mice with a re-assorted virus carrying the HA segment of PR8F in the genetic background of PR8M showed that indeed the HA gene is the major determinant for lethality.

Results

Higher propagation rates and enhanced spread into alveolar regions in the lungs of DBA/2J mice after infection with PR8M virus

We previously showed that DBA/2J mice were much more susceptible to the PR8M influenza virus variant than C57BL/6J mice (Srivastava et al., 2009). The extremely high susceptibility of DBA/2J mice was associated with a higher replication rate in the lungs of DBA/2J compared to C57BL/6J mice (Srivastava et al., 2009). We now expanded these studies by analyzing earlier time points after infection and performing semi-quantitative analysis of infected cells in histological sections. All infections were performed at an infection dose of 2×10^3 FFU. At this dose, different mouse strains exhibited differential responses to the low pathogenic variant PR8M (Srivastava et al., 2009) and it was thus considered to represent an appropriate dose to determine differences in pathogenicity of different virus variants.

At 12 h post infection (p.i.), PR8M titers in the lungs of infected DBA/2J mice reached 1×10^4 FFU whereas virus titers in infected C57BL/6J mice were below the detection limit (Fig. 1). These observations suggest a cell intrinsic difference in the binding or replication capacity of respiratory epithelial cells in DBA/2J mice compared to C57BL/6J. The higher viral loads in DBA/2J mice at early time points p.i. could either be due to a higher replication rate of the virus in infected cells or may be the result of a higher number of cells infected. To address this question, we examined paraffin sections from

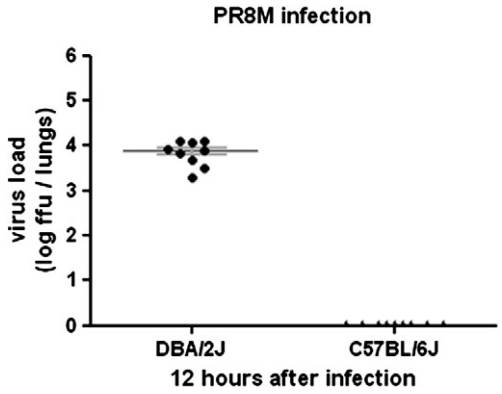

Fig. 1. PR8M reproduced to high levels in the lungs of DBA/2J mice but not in C57BL/6J mice at early time points after infection. Nine DBA/2J and C57BL/6J mice were infected intra-nasally with a dose of 2×10^3 FFU of PR8M virus and viral load in the lungs was measured at 12 h p.i. by focus formation assay. At this time point, the amounts of infectious particles in C57BL/6J mice were below the level of detection. For DBA/2J mice the mean values ± SEM are shown.

PR8M infected lungs of DBA/2J and C57BL/6J mice and counted the number of infected cells in the bronchiolar and alveolar regions after immune-histochemical staining of the viral nucleoprotein (NP). In the lungs of DBA/2J mice, virus-infected cells were present both in the

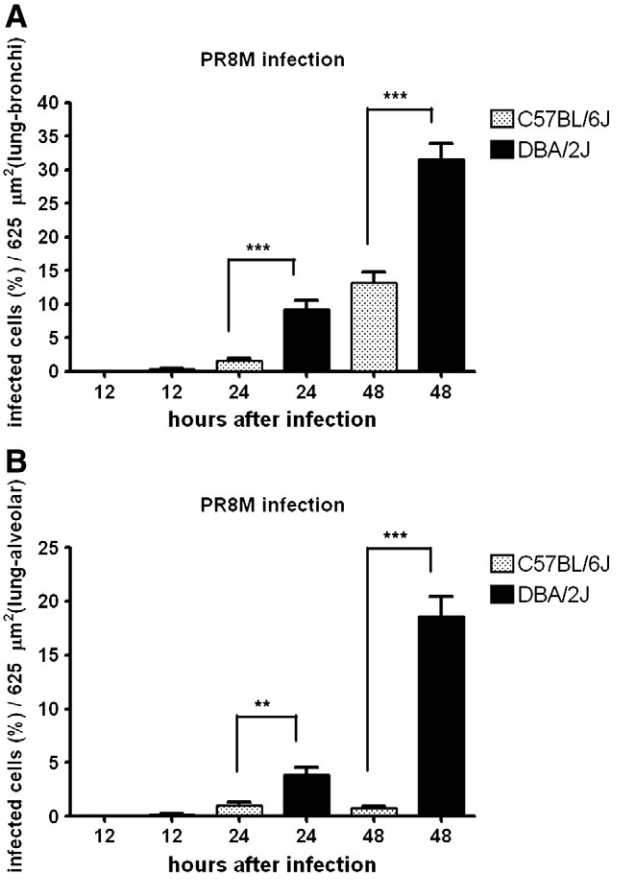

Fig. 2. The number of infected cells and spreading of PR8M virus into alveolar regions was higher in DBA/2J compared to C57BL/6J mice. Three DBA/2J and three C57BL/6J mice were infected intra-nasally with 2×10^3 FFU of PR8M viruses. Three lung sections from each mouse (total of nine sections per mouse strain) were stained with anti-influenza NP antibody and haematoxylin. The numbers of infected cells in bronchiolar (A) and in alveolar (B) regions were calculated per 625 µm² total surface of lung tissues after 12, 24 and 48 h p.i. Mean values ± SEM are shown. DBA/2J and C57BL/6J mice were compared for statistical significant differences using non-parametric Mann–Whitney-U-test. **: p value<0.01; ***: p value<0.001.

bronchiolar and alveolar regions already at 12 h p.i., whereas in C57BL/6J mice no infected cells were detected at this time point (Fig. 2). At later times p.i. significantly higher numbers of infected cells were observed in DBA/2J mice compared to C57BL/6J mice in both bronchiolar (Fig. 2A) and alveolar regions (Fig. 2B). Most remarkably, the virus did spread into alveolar regions much earlier and to a significantly higher level in DBA/2J compared to C57BL/6J mice (Fig. 2B). Fig. 3 shows examples of histological pictures illustrating the rapid spread of PR8M virus into the alveolar regions of DBA/2J mice. In conclusion, these observations not only demonstrated that a higher number of cells was infected in DBA/2J compared to C57BL/6J mice but also that the virus did spread more deeply into the alveolar regions of the lungs in DBA/2J mice. This enhanced spread is most likely the reason for the high mortality rate in DBA/2J mice.

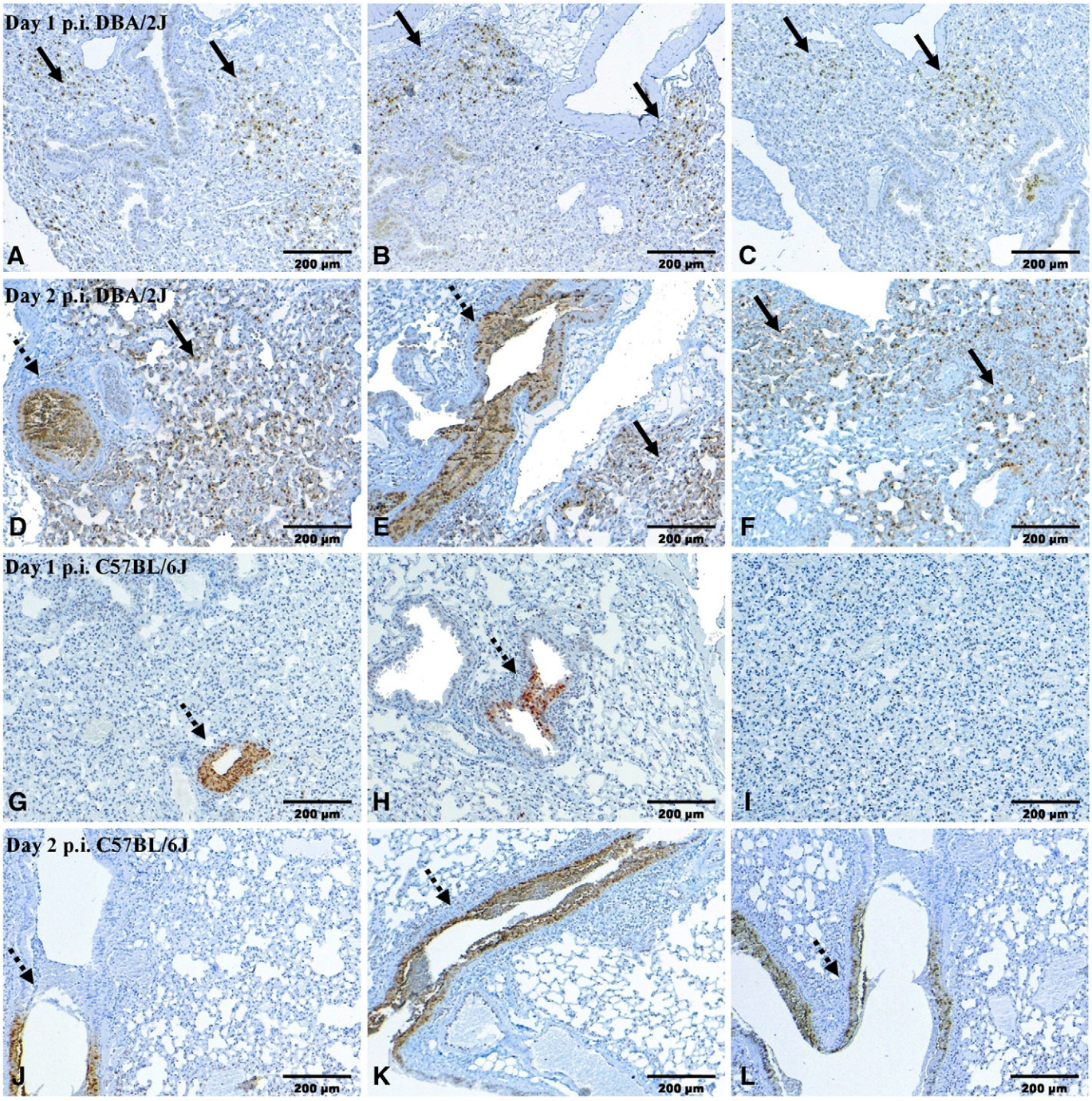

Fig. 3. Histological sections of lungs from DBA/2J and C57BL/6J mice infected with PR8M virus. PR8M infected cells were observed in bronchiolar and alveolar regions in the lungs of DBA/2J mice. DBA/2J (A–F) and C57BL/6J (G–L) mice were infected intra-nasally with 2×10^3 FFU of PR8M virus. Serial lung sections were stained with anti-influenza NP antibody and haematoxylin. Already at day 1 p.i., large patches of virus-infected cells (brown staining) were found in DBA/2J mice in alveolar regions (solid arrows, A–C) in addition to infected bronchiolar regions (not shown). At day 2 p.i., PR8M infected cells could be detected throughout the lungs in DBA/2J mice, both in bronchiolar (dashed arrows, D–E) and in alveolar regions (solid arrows, D–F). In C57BL/6J lungs, the spread of PR8M virus (cells stained brown) at day 1 (G–I) and day 2 (J–L) p.i. was mostly limited to bronchiolar regions (dashed arrows). Scale bars represent 200 µm.

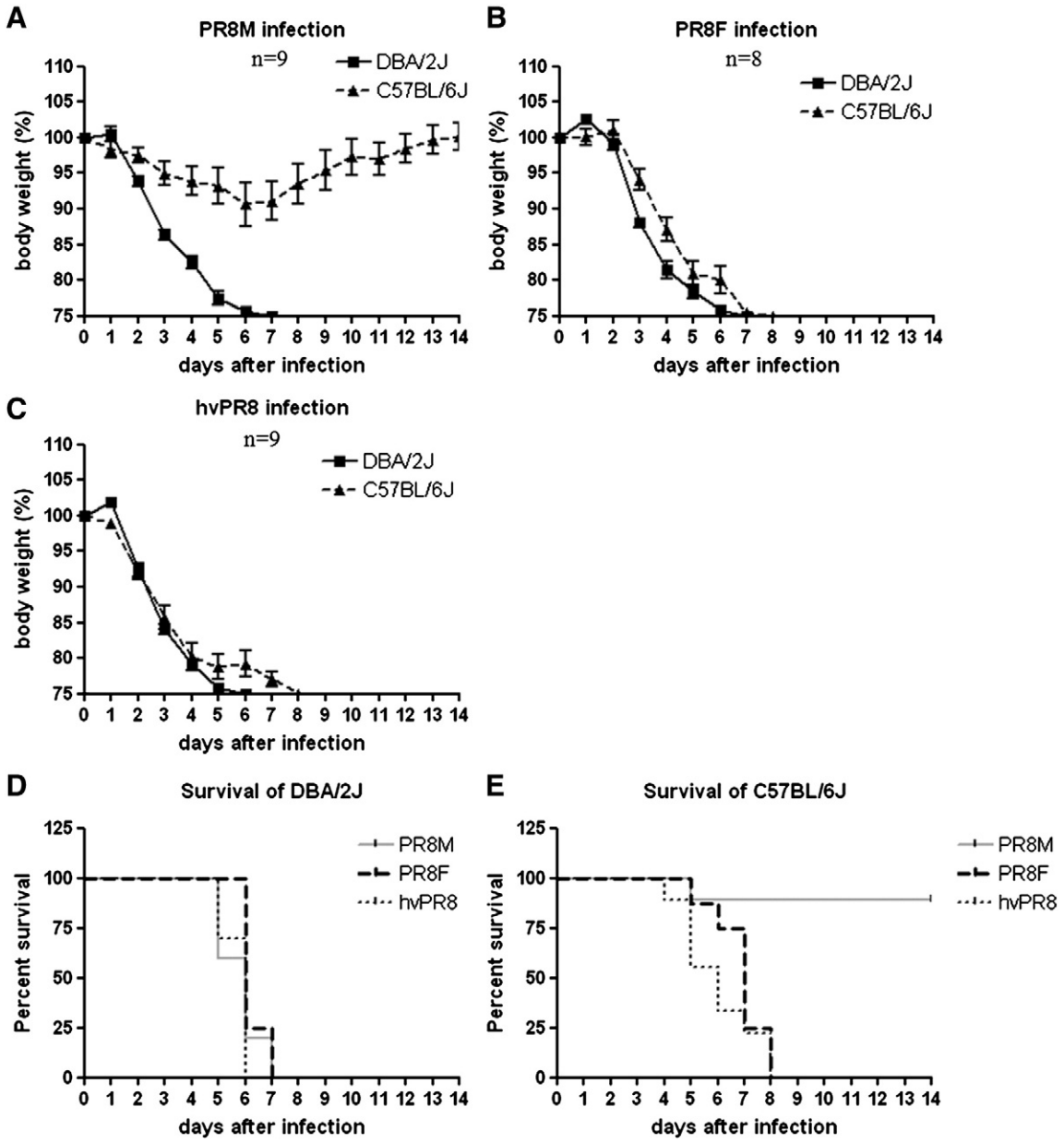

Fig. 4. Difference in the susceptibility of DBA/2J and C57BL/6J mice to infections with PR8M, PR8F and hvPR8 virus variants. DBA/2J and C57BL/6J mice were infected intra-nasally with 2×10^3 FFU PR8M (A), PR8F (B) or hvPR8 (C) and weight loss was monitored over a 14-day period. For comparison, also previously published data (modified from (Srivastava et al., 2009) for weight loss and survival of DBA/2J and C57BL/6J mice infected with the PR8M variant was included (A, D, E). Mean percent of body weight change (±SEM) is shown, and n refers to the total number of mice from two independent experiments infected in each group. Survival of DBA/2J mice is shown in (D) and of C57BL/6J mice in (E). Mortality also included mice that were sacrificed because they had lost more than 25% of body weight.

PR8F and hvPR8 virus variants are similarly pathogenic for both DBA/2J and C57BL/6J mice and replicate to comparable levels

Next, we infected DBA/2J and C57BL/6J mice with two additional PR8 variants, PR8F and hvPR8 which were described to be also lethal for C57BL/6J mice (Grimm et al., 2007). As shown in Figs. 4A and B, the kinetics of weight loss and survival of DBA/2J and C57BL/6J infected with PR8F and hvPR8 were largely similar (Figs. 4B, C) which is in contrast to the results observed for PR8M where DBA/2J mice were much more susceptible (Fig. 4A). In DBA/2J mice, viral loads were similar after infection with PR8M (Fig. 5A) and PR8F (Fig. 5B) and even higher after infection with hvPR8 (Fig. 5C). In C57BL/6J mice, viral load was lower than in DBA/2J mice after infections with PR8M virus (Fig. 5A). However, viral loads were similarly high in C57BL/6J and DBA/2J mice after infection with PR8F or hvPR8 virus (Figs. 5B, C). Thus, the differences in viral loads correlated well with the severity of weight loss and mortality for all three virus variants in the two mouse strains studied. These data suggest that a continuously high viral load (above 10^5 FFU) will lead to severe tissue damage, lung dysfunctions and subsequent death.

In histological sections of mice infected with PR8F and hvPR8, many virus infected cells could be detected in alveolar regions, both in C57BL/6J and in DBA/2J mice at days 1 and 2 after infection (Fig. 6). This is in contrast to PR8M infections where NP-positive cells were mostly restricted to bronchiolar regions in C57BL/6J mice (Figs. 3G–L). These observations demonstrated again that the virulence of the different PR8 variants correlated well with the capability of the virus to replicate in alveolar regions, suggesting that penetration of influenza virus into these deeper regions of the lung is a major determinant of a lethal pathology.

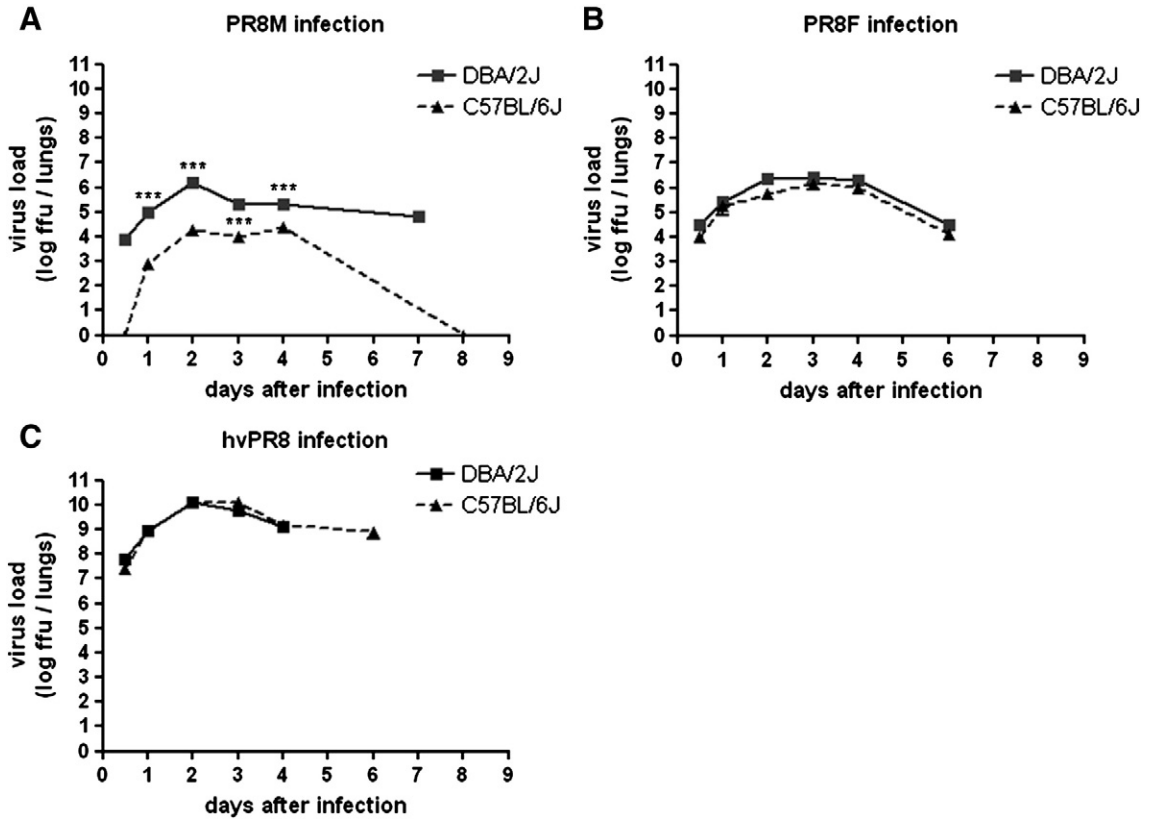

Fig. 5. PR8F and hvPR8 reproduced to similar levels in the lungs of DBA/2J and C57BL/6J mice. DBA/2J and C57BL/6J were infected intra-nasally with 2×10^3 FFU of PR8M (A), PR8F (B) or hvPR8 (C) and viral load in the lungs was measured at indicated times p.i. using focus formation assay. For comparison, also previously published data (modified from Srivastava et al., 2009) on the viral load in the lungs of DBA/2J and C57BL/6J after infection with the PR8M variant was included (A). Six DBA/2J and six C57BL/6J mice were used for all time points. Mean values ± SEM from a total of two independent experiments are shown. DBA/2J and C57BL/6J mice were compared for statistical significant differences using non-parametric Mann–Whitney-U-test. ***: p value < 0.001.

Higher viral load in C57BL/6J mice is accompanied with a stronger leukocyte infiltration

Besides the viral load, also the strength of the inflammatory immune response is thought to contribute to the severity of disease. In particular, deleterious inflammatory responses have been suggested in the context of lethal H5N1 infections in humans and animals. Therefore, we investigated the degree of immune cell infiltration in C57BL/6J mice infected with PR8M and PR8F, since viral loads in C57BL/6J mice were different after infection with these two variants. As shown in Fig. 7, at day 1 p.i. similarly low numbers of infiltrating leukocytes were observed after infection with both viruses and in non-infected controls. At day 2 p.i., a slightly higher number of infiltrates was observed in PR8F infected mice, but at day 3 p.i. a significantly higher number of infiltrating cells was observed in PR8F compared to PR8M infected mice (Fig. 7). Thus, a higher inflammatory response was correlated with high viral load and a more severe lung pathology. It should, however, be noted that such a strong link between viral load and inflammatory response may not always be observed. In particular, such a correlation may not be apparent when more distantly related virus subtypes are compared or when mice are infected that are genetically different by mutation or have been treated with anti-inflammatory drugs.

Differences in the HA amino acid sequence may account for different protein folding and protease cleavage in the PR8F versus PR8M variant

The PR8M and PR8F were obtained from two different laboratories and were not previously compared directly. Here, we observed a significantly different pathogenicity of PR8M and PR8F in C57BL/6J mice. To obtain further insights into the molecular basis of these differences, we sequenced all viral segments from both viruses. Several differences in the predicted amino acid sequences were observed in various viral segments.

The predicted amino acid sequence of the HA gene exhibited six amino acid changes between PR8F and PR8M (S10C, S123R, G276D, M288I, T337I and I349F, respectively). The most frequently observed amino acids at these positions are (data from Influenza Research Database (IRD, http://www.fludb.org/brc/home.do?decorator=influenza)): 10 C, S123, G276, M288, 337I, I349. Thus, the positions 123, 276, 288 and 349 in PR8M differ from this consensus and most likely account for the difference in virulence between PR8F and PR8M. Most of the changes resided in the HA1 region, only I349F was at the beginning of HA2 just after the cleavage site. T337I and I349F surrounded the cleavage site. There were no changes observed in the predicted fusion peptide itself and no amino acid differences were found which would predict a difference in glycosylation. Modeling of the potential influence of the variation in amino acids at positions T337I and I349F suggested a difference in HA folding (Fig. 8) in a loop formed by amino acids 335 to 351. This structural change may enable the cleavage peptide in the PR8F HA to be more exposed and thus to fit better into the active site of trypsin-like proteases. Therefore, these alterations in PR8F may allow for better processing of the HA by host proteases and thereby render this variant more infectious.

In the predicted NA protein sequence, two amino acid differences were observed between PR8F and PR8M, at positions 8 and 131. The predicted PA sequences showed two difference at positions 11 and 15, the predicted NP sequence revealed three amino acid differences at positions 7, 12 and 496, the predicted PB1 sequences showed four differences at positions 2, 7, 10 and 436, and the predicted PB2 sequence showed one amino acid difference at position 4. No differences were observed in the NS and M gene segments. For all

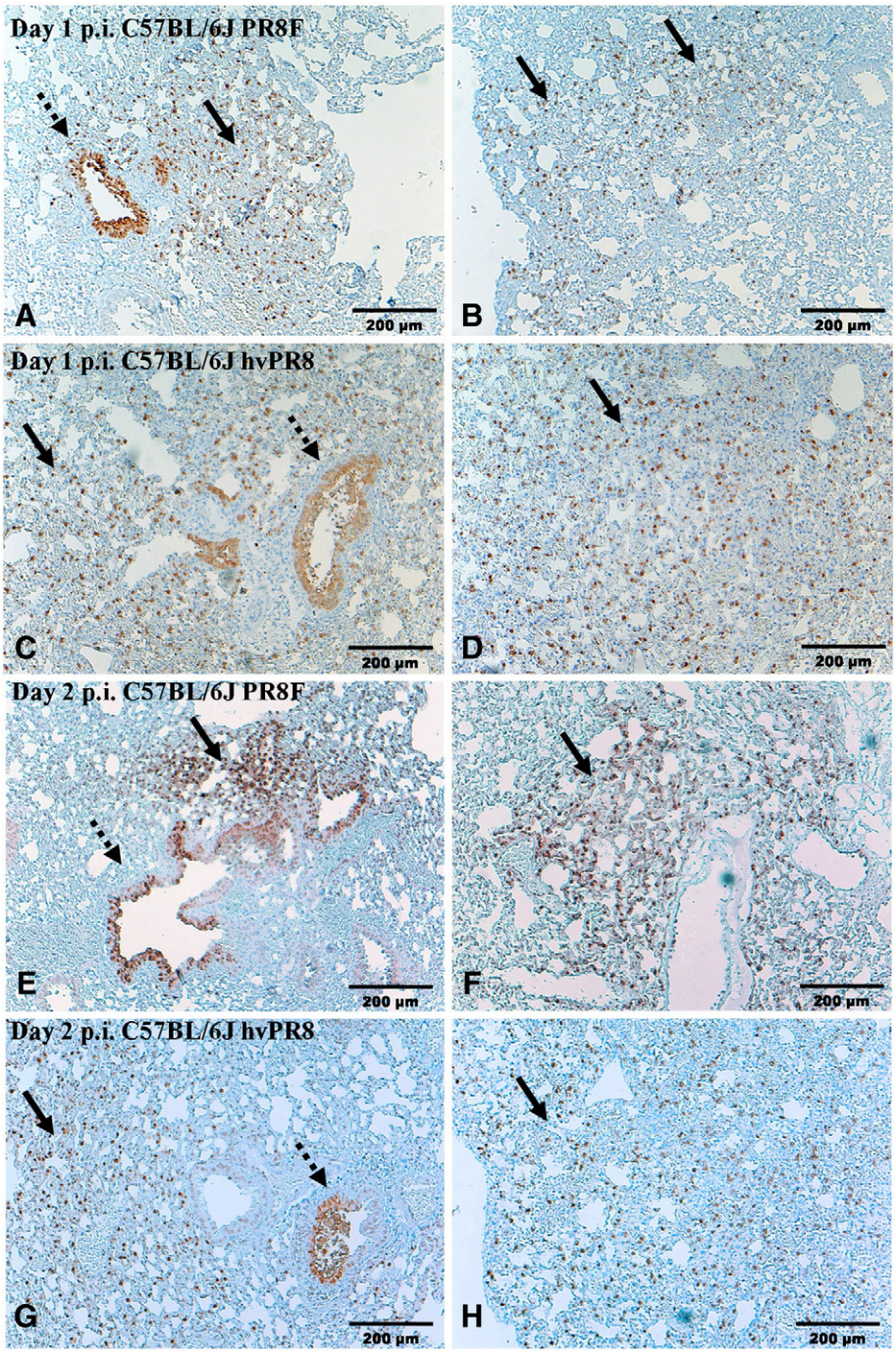

Fig. 6. Histological sections of lungs from C57BL/6J mice infected with PR8F and hvPR8 virus variants. Three C57BL/6J mice (per virus variant) were infected intra-nasally either with 2×10^3 FFU of PR8F (A,B,E,F) or hvPR8 (C,D,G,H). Serial lung sections were stained with anti-influenza NP antibody and haematoxylin. At day 1 p.i., large areas of virus-infected cells (brown staining) were found in alveolar regions (solid arrows in A, B) in addition to infected bronchiolar regions (dashed arrow, A) of C57BL/6J mice infected with PR8F. Similarly, at day 1 p.i., C57BL/6J mice infected with hvPR8 presented NP-positive cells in alveolar (solid arrows, C,D) and bronchiolar regions (dashed arrow, C) with slightly more alveolar regions infected compared to PR8M infected mice. At day 2 p.i., PR8F (E,F) and hvPR8 (G,H) infected cells could be detected throughout the lungs of C57BL/6J mice, both in bronchiolar (dashed arrows, PR8F-E, hvPR8-G) and in alveolar regions (solid arrows, PR8F in E,F and hvPR8 in G,H). Scale bars represent 200 µm.

amino acid differences, the PR8M sequence represented the variant which was most common to all sequenced H1N1 viruses in the IRD.

The HA segment is the main determinant for the high virulence of the PR8F virus variant

To determine whether the HA segment indeed accounts for the difference in virulence between the PR8M and PR8F variants, we generated a genetic re-assortant (PR8M-HA-F) which contained the HA fragment of the PR8F variant in the background of the PR8M virus. As shown in Fig. 9, survival was much lower and significantly different ($p<0.01$, log rank test) for PR8M-HA-F compared to PRM infected C57BL/6J mice. Only 20% of PR8M-HA-F infected mice survived whereas all mice survived an infection with PR8M virus. On the other hand, survival was slightly but significantly ($p<0.01$, log rank test) higher for PR8M-HA-F compared to PR8F infected mice. These results demonstrated that the HA segment is indeed the main determinant of the high virulence of the PR8F variant.

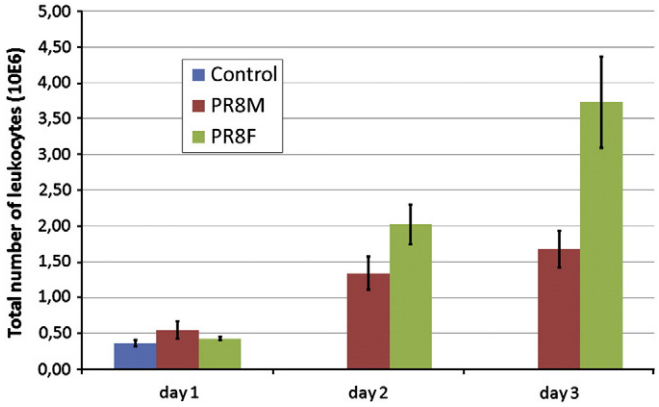

Fig. 7. Lung infiltrates correlate with viral load and severity of disease. Infiltrating immune cells were isolated from mouse lung homogenates and analyzed by FACS by staining for CD45 expression. The number of infiltrating CD45-positive cells was determined for days 1 to 3 after infection with either PR8M or PR8F virus. Non-infected mice were used as control. The number of infiltrates at days 2 and 3 p.i. were significantly higher in infected compared to control (uninfected) mice ($p<0.01$ for both days, using non-parametric Kruskall–Wallis test). Infiltrates in both PR8M and PR8F infected mice changed significantly over time ($p<0.05$ and $p<0.01$ respectively using non-parametric Kruskall–Wallis test). The amount of infiltrates at day 3 p.i. was significantly higher ($p<0.01$ using Mann–Whitney-U-test) in mice infected with PR8F than in mice infected with PR8M (B). Mean values ± SEM are shown of $n=5$ mice for control and days 1 or 2 and $n=4$ mice for day 3. One of two experiments with similar results is shown.

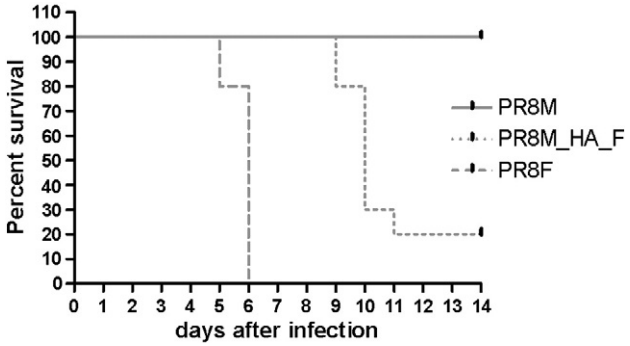

Fig. 9. The re-assorted virus PR8M-HA-F virus is highly lethal for C57BL/6J mice. Ten C57BL/6J mice (for each virus variant) were infected intra-nasally with each 2×10^3 FFU PR8M, PR8M-HA-F or PR8F and survival was monitored over a 14-day period. Infection with PR8M-HA-F virus resulted in high mortality which was significantly different to the survival rate of PR8M infected mice ($p<0.01$ using log rank test). Mortality also included mice that were sacrificed because they had lost more than 25% of body weight.

Discussion

The outcome of an infection is the result a complex interplay between the virulence of the pathogen and the host response. Both are influenced by environmental but also to a large extent by genetic factors. Here, we studied the host–pathogen-interactions for three different variants of a mouse-adapted influenza virus, PR8: a low pathogenic variant PR8M, a highly pathogenic variant PR8F which is lethal to mice at intermediate doses of infection, and a very highly pathogenic variant hvPR8 which is lethal even at low doses of infection (Grimm et al., 2007; Srivastava et al., 2009). The host response was investigated in two different mouse strains: the DBA/2J mouse strain being highly susceptible to all three virus variants and the C57BL/6J mouse strain showing differential susceptibility depending on the virus variant.

DBA/2J mice were susceptible to all three PR8 virus variants exhibiting dramatic weight loss after infection with 2×10^3 FFU, and

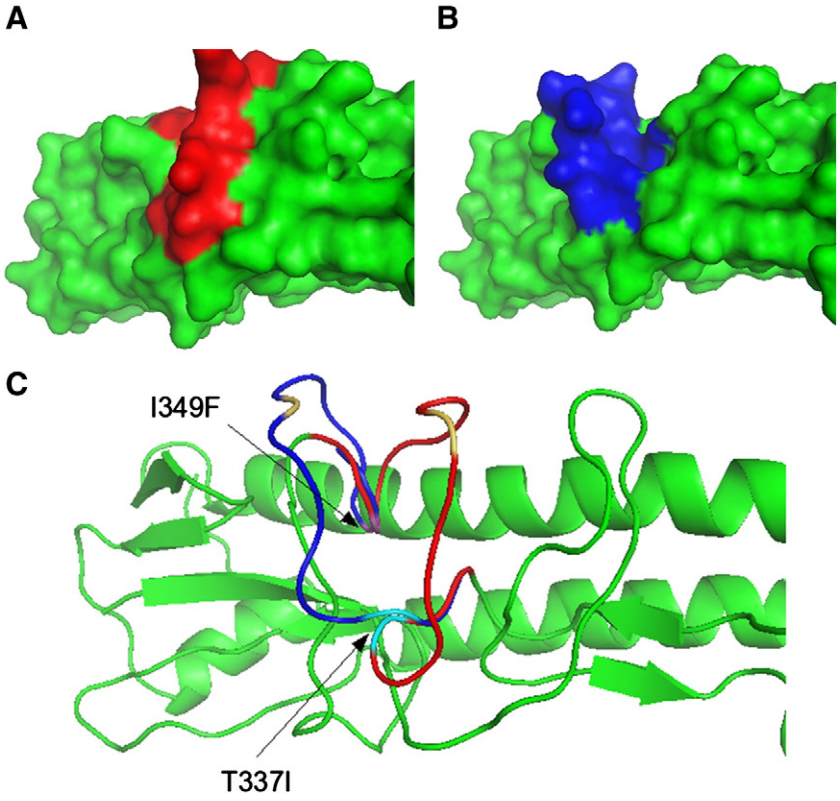

Fig. 8. Two-amino acid changes near the HA cleavage side predict better exposure of the protease cleavage site of the HA in PR8F. The three-dimensional structures of the HA proteins from PR8M and PR8F were modeled and compared. The surface model of the region between residues 337 and 349 in the loop of the PR8M variant was predicted to be closer to the surface of the rest of the protein (A, red) and may therefore be less available to fit into the pocket of the host proteases. The surface model of this region in the PR8F variant (B, blue) was predicted to be better exposed and may thus exhibit a better interaction with host proteases. The protease cleavage site is shown in yellow in the ribbon model in (C). The HA cleavage site peptide of PR8M is shown in blue, the cleavage site peptide in PR8F in red. The amino acid T337I is marked in cyan and I349F in violet (solid arrows, C).

infections with all three virus variants mice were lethal for DBA/2J mice. C57BL/6J mice showed a differential response. While they survived infections with the low pathogenic PR8M, they succumbed to both the PR8F and hvPR8 variant. Analysis of virus propagation in the lung showed that the lethal outcome strongly correlated with a high viral load. DBA/2J mice exhibited a much higher viral load compared to C57BL/6J mice when infected with the low virulent PR8M variant. In contrast viral loads after infection with the PR8F variant were similarly high in C57BL/6J and DBA/2J infected mice. For the very high virulent virus hvPR8 it has been previously shown that it replicates to a much higher rate compared to other influenza virus isolates (Grimm et al., 2007). Consistent with these findings we also observed the highest replication rates in hvPR8 infected mice, with DBA/2J and C57BL/6J exhibiting similar levels of virus in their lungs. DBA/2J mice were also shown to exhibit a higher susceptibility compared to C57BL/6J mice when infected with other influenza A virus subtypes (Boon et al., 2010; Srivastava et al., 2009).

Taken together, our results suggest that there might be a tolerable threshold of virus propagation in the lungs of infected animals below which viral reproduction is not lethal whereas above this threshold enhanced damage in respiratory epithelia occurs. The high viral reproduction thus leads to irreversible pathologies of the lung and a fatal outcome, especially if the virus is spreading into the alveolar regions. In our experiments this threshold appeared to be between 10^5 and 10^6 viruses per lung for infections with mouse-adapted PR8 virus. The importance of a threshold in virus titers was shown to play a role in infections with H5N1 influenza virus (Hatta et al., 2010) and also in the outcome of Simian Immunodeficiency Virus and Simian–Human Immunodeficiency Viruses (Ten Haaft et al., 1998) as well as Lassa Virus (Baize et al., 2009) in monkeys.

It should also be noted, that several studies have shown that the host immune response is an important factor in the severity of influenza-induced pathology. Infection-associated hyper-inflammatory responses may contribute to tissue damage and pathogenicity with lethal outcomes (Aldridge et al., 2009; de Jong et al., 2006; Herold et al., 2008; Kash et al., 2006; La Gruta et al., 2007; Perrone et al., 2008; Tumpey et al., 2005). Inhibition of strong inflammatory responses, e.g. by anti-inflammatory drugs was shown to result in improved survival even when viral loads were unaltered (Aldridge et al., 2009; Budd et al., 2007; Palamara et al., 2005; Zheng et al., 2008). Here, we observed higher leukocyte infiltrates after infection with the highly virulent PR8M compared to the less virulent PR8M virus variant in C57BL/6J mice. These results demonstrate that there is a stronger inflammatory response during lethal infections.

After administration of low virulent PR8M virus in DBA/2J mice, the viral loads were already very high at 12 h p.i. and more cells were infected in DBA/2J lungs, compared to PR8M infections in C57BL/6J mice. However, at later time points, the slope of increase in viral loads was similar for both mouse strains. This high permissiveness of virus reproduction for the low virulent PR8M virus in DBA/2J mice, especially at early time point p.i. could be explained in several ways. First, DBA/2J mice may exhibit a higher number of receptors allowing more cells to be infected. Second, the uptake of virus and transport to the nucleus is more efficient in DBA/2J mice. Third, assembly or release of the virus from infected cells is more efficient in DBA/2J mice. Forth, the innate immune response is less efficient in DBA/2J mice. We are currently addressing these hypotheses in more detail in lung organ cultures.

DBA/2J mice do not show any overt signs of a general deficiency in the early innate immune response because no abnormalities were observed in the activation of inflammatory response genes (Alberts et al., 2010) or production of chemokines and cytokines (Srivastava et al., 2009). Furthermore, differences in the replication rates of influenza virus within infected cells are less likely to account for this difference in viral load because the slope of the increase in virus replication over time was similar in both mouse lines. Also, infections of both mouse strains with the more virulent PR8F variant produced similar amounts of infectious virus in infected lungs suggesting that host factors required for viral reproduction are not generally more supportive in DBA/2J mice.

We then looked in more detail at the structural differences between the PR8M and PR8F variants. Both variants are closely related derivatives of the PR8 Mount Sinai strain but exhibited differences in the predicted amino acid sequences in several viral proteins. The most notable differences were found in the predicted HA sequence. The HA sequence differed in six amino acids that were not located in the receptor binding site. However, two amino acid differences surrounded the protease cleavage site which is involved in processing of the HA0 precursor into the two functional subunits HA1 and HA2. Modeling of the 3D-structure of the HA sequences from the two PR8 variants suggested that the differences in the HA of PR8F may lead to structural changes which would allow a better interaction of the protease cleavage site with host trypsin-like proteases. We hypothesize that this structural change may result in a more efficient processing of the PR8F HA and subsequently would allow a faster spread of the virus.

Indeed, the low survival rate of mice infected with a genetic re-assortant carrying the HA encoding segment of the PR8F virus in the background of the PR8M virus (PR8M-HA-F) demonstrated that the HA protein is the main determinant of the higher virulence of the PR8F virus. Although clearly more virulent than the PR8M virus, the re-assorted PR8M-HA-F virus did not result in the same mortality rate as the PR8F virus suggesting that some of the other viral segments which differ between PR8F and PR8M may further contribute to the higher virulence of PR8F.

Materials and methods

Viruses

PR8M and PR8F variants are closely related to the Mount Sinai strain of A/PR/8/34 (H1N1). They were generated by serial lung passages in *Mx1*$^{-/-}$ mice and are referred to as “low pathogenic” viruses (Schickli et al., 2001). Original stocks of the variant PR8M (initially generated from plasmids kindly provided by Erich Hoffmann, Memphis, TN, USA) were taken from the strain collection at the Institute of Molecular Virology, Muenster, Germany. The PR8F variant was provided by Peter Staeheli, Department of Virology, Freiburg, Germany. The hvPR8 (“highly virulent” PR8) variant is closely related to the Cambridge strain of A/PR/8/34 (H1N1) (Grimm et al., 2007) and was generated by serial passages in *Mx1*$^{+/+}$ mice. The original stock was also provided by Peter Staeheli. Virus stocks were propagated in the chorio-allantoic cavity of ten days old pathogen-free embryonated chicken eggs for 48 h at 37 °C. PR8M-HA-F virus was generated and propagated on HEK293 and MDCK cells as described by (Hoffmann et al., 2002). The HA segment of recombinant PR8M-HA-F virus was sequenced after reverse transcription PCR amplification from infected cells to verify the presence of the desired re-assorted HA gene.

Mouse strains and infections

DBA/2J and C57BL/6J mice were purchased from Janvier, France. Mice were maintained under specific pathogen free conditions and according to the German animal welfare law. All experiments were approved by an external committee according to the German regulations on animal welfare. Animals (10–11 weeks of age) were anesthetized by intra-peritoneal injection of Ketamine–Rompun with a dose adjusted to the individual body weight and infected intra-nasally with the specified dose of virus in 20 μl of sterile PBS. Weight loss and survival of infected mice were monitored over a 14-day period. Animals showing more than 25% of body weight loss were euthanized and documented as dead.

Determining infectious viral particles

Virus titers were determined on MDCK II (Madin–Darby Canine Kidney II) cells using the focus formation (FOCI) assay. Briefly, MDCK II cells (6×10^4 cells/well) were seeded in 96-well culture plates and incubated at 37 °C in 5% CO_2 for 24 h. Serial 10-fold dilutions of extracts were prepared in DMEM containing 2.5 μg/ml NAT (N-Acetylated Trypsin, Sigma), 0.1% BSA, 1% penicillin/streptomycin and added to MDCK II cells. After 1 h of incubation at 37 °C in 5% CO_2, the inoculates were replaced with 100 μl of 1% Avicel overlay prepared in DMEM containing 2.5% NAT, 0.1% BSA and the cells were incubated for 24 h. Subsequently, the cells were washed twice with PBS and fixed with 4% formalin in PBS (100 μl/well) for 10 min at room temperature. Then, the cells were washed twice and incubated with Quencher (100 μl/well; 0.5% Triton X-100, 20 mM Glycine in PBS) for 10 min at room temperature. Subsequently, the cells were washed with Washing Buffer WB (100 μl/well; 0.5% Tween20 in PBS) and blocked with Blocking Buffer BB (50 μl/well; 0.5% Tween, 20% BSA in PBS) for 30 min at 37 °C in 5% CO_2. The primary antibody (anti-influenza Nucleocapsid NP polyclonal goat antibody, Virostat) and the secondary antibody (anti-goat-HRP from KPL, MA, USA) were diluted 1:1000 in Blocking Buffer (BB). 50 μl of the primary antibody was added to each well and incubated for 1 h at room temperature. After 1 h, the cells were washed three times with Washing Buffer WB, incubated with 50 μl of secondary antibody for 45 min in the dark, then washed again and incubated with 50 μl of substrate (True Blue from KPL, MA, USA) and exposed until blue spots from infected cells appeared (about 10 min). Foci were counted and viral titers were calculated as focus formation units (FFU) per ml of lung homogenate, lung slice homogenate or supernatant collected from the lung slice.

Immunohistochemistry and quantification of infected cells in lungs

Lung tissues were prepared and immersion-fixed for 24 h in 4% buffered formaldehyde solution (pH 7.4), dehydrated in a series of graded alcohols and embedded in paraffin. Sections (0.5 μm) were cut with the microtome (Microm HM340E). Subsequently, the lung sections were stained overnight at with the primary antibody (anti-influenza Nucleoprotein NP polyclonal goat antibody, Virostat) at 4 °C. Then, tissue sections were incubated for 30 min with the secondary antibody (rabbit anti-goat-biotin from KPL, MA, USA). The primary and secondary antibodies were diluted 1:800 and 1:250 respectively. Finally, the sections were slightly counterstained with haematoxylin to facilitate the localization of bronchiolar and alveolar regions. Histological sections were examined and the infected cells were counted using an ocular with counting squares corresponding to a 25×25 μm area in combination with a 40× objective. In total, 50 areas were investigated per lung, 10 in each lobe. For this, the 25×25 μm square was moved over the sections and the cells in every second interval were analyzed. For each day and each infected mouse strain, three replicates were analyzed. All cells which showed positive NP staining, irrespective of its intracellular location, were scored.

Flow cytometry and determination of infiltrating lymphocytes

Mice were sacrificed by CO_2 inhalation, the inferior vena cava was cut and the lung perfused by injecting 10 ml of PBS into the heart. Subsequently, lungs were disrupted mechanically using a 100 μm cell strainer (BD Falcon) and the piston of a syringe. The cell suspension was centrifuged and the pellet resuspended in FACS buffer (PBS + 2% Fetal Bovine Serum + 2 mM EDTA). The total number of life cells was determined after staining with 0.4% trypan blue in a hemocytometer. The trypan-negative cells were considered as life cells. The cell pellet was resuspended to a concentration of 1×10^6 cells/100 ml. Staining with antibodies was performed by first blocking the Fc receptors using a anti-CD16/32 antibody for 15 min at 4 °C. Then, the cells were centrifuged, washed in FACS buffer and stained in 100 ml of CD45.2 (104) antibody solution for 30 min at 4 °C. Cells were centrifuged, washed and resuspended in 100 μl FACS buffer for acquisition. Propidium Iodide solution (PI) was added just before the measurement on a LSRII FACS machine from BD. The results were analyzed with the BD DIVA software. The total number of leukocytes in the lung (TL) was calculated by multiplying the number of $CD45.2^+PI^-$ events ($CD45.2^+$) with the total number of live cell counts determined by trypan exclusion (CC), divided by the total PI^- events (PI^-): $TL = (CD45.2^+ \times CC)/PI^-$.

Haemagglutinin protein structure prediction

Amino acid sequences of HA from PR8F and PR8M was aligned and edited using ClustalW and BioEdit. Protein three-dimensional structures were obtained from RCSB PDB (Protein Data Bank; http://www.rcsb.org). The octamer (PDB CODE: 1RU7) was dissociated into the monomeric structure of the HA1/HA2 complex and was applied for further investigation. SWISS MODEL server (http://www.swissmodel.expasy.org) was used to model the structures of HA proteins. The quality of the resulting data and the likeness of protein structure predictions were evaluated using METAMQAP method (https://genesilico.pl/toolkit/unimod?method=MetaMQAPII). The loops of the HA proteins were improved with RefinerLoop method (https://genesilico.pl/toolkit/unimod?method=RefinerLoop). From the 20 top-scoring models verified with METAMQAP the best scored model was chosen.

Data analysis

Data were analyzed using GraphPad Prism version 5.00 for Windows (GrahpPad Software, San Diego, California; http://www.graphpad.com). Mean ± SEM were calculated for percent body weights, viral titers and number of virus-infected cells in the histology slides. The non-parametric Mann–Whitney-U-test was used to determine p-values for the significance of differences between groups. P-values of ≤0.05 were considered significant. For comparisons of survival curves, a log rank test was performed using the online tool provided by http://www.bioinf.wehi.edu.au/software/russell/logrank/.

Author contributions

PB designed and performed the experiments and wrote the manuscript. LK performed the structural predictions of the PR8M and PR8F proteins. NV performed the immune cell infiltration studies together with PB. KS designed the experiments and wrote the manuscript. DA generated the isogenic PR8M-HA-F virus supervised by SL who contributed to manuscript writing.

Acknowledgments

This work was supported by intra-mural grants from the Helmholtz-Association (Program Infection and Immunity) and a research grant FluResearchNet (No. 01KI07137) from the German Ministry of Education and Research to KS. PB was supported by the Georg-Christoph-Lichtenberg-Foundation. We are very grateful to Erich Hoffmann, Memphis, TN, USA, for providing the eight plasmid systems (pHW2000 191-198 A/PR8/34) for generation of the recombinant PR8M virus as well as the PR8M-F-HA re-assortant. PR8F and hvPR8 variants were obtained from Peter Staeheli (Department of Virology, Freiburg, Germany). The plasmid of the PR8F-HA segment used to produce reassortant PR8M-F-HA was provided by Georg Kochs (Department of Virology, Freiburg, Germany). We thank Christin Fricke and Anna Rinkel for excellent

technical support. Mice for these experiments were maintained by the animal caretakers of the Central Animal Facilities at the HZI.

References

Alberts, R., Srivastava, B., Wu, H., Viegas, N., Geffers, R., Klawonn, F., Novoselova, N., do Valle, T.Z., Panthier, J.J., Schughart, K., 2010. Gene expression changes in the host response between resistant and susceptible inbred mouse strains after influenza A infection. Microbes Infect. 12 (4), 309–318.

Albright, F.S., Orlando, P., Pavia, A.T., Jackson, G.G., Cannon Albright, L.A., 2008. Evidence for a heritable predisposition to death due to influenza. J. Infect. Dis. 197 (1), 18–24.

Aldridge Jr., J.R., Moseley, C.E., Boltz, D.A., Negovetich, N.J., Reynolds, C., Franks, J., Brown, S.A., Doherty, P.C., Webster, R.G., Thomas, P.G., 2009. TNF/iNOS-producing dendritic cells are the necessary evil of lethal influenza virus infection. Proc. Natl Acad. Sci. USA 106 (13), 5306–5311.

Baize, S., Marianneau, P., Loth, P., Reynard, S., Journeaux, A., Chevallier, M., Tordo, N., Deubel, V., Contamin, H., 2009. Early and strong immune responses are associated with control of viral replication and recovery in lassa virus-infected cynomolgus monkeys. J. Virol. 83 (11), 5890–5903.

Belser, J.A., Lu, X., Maines, T.R., Smith, C., Li, Y., Donis, R.O., Katz, J.M., Tumpey, T.M., 2007. Pathogenesis of avian influenza (H7) virus infection in mice and ferrets: enhanced virulence of Eurasian H7N7 viruses isolated from humans. J. Virol. 81 (20), 11139–11147.

Belser, J.A., Wadford, D.A., Pappas, C., Gustin, K.M., Maines, T.R., Pearce, M.B., Zeng, H., Swayne, D.E., Pantin-Jackwood, M., Katz, J.M., Tumpey, T.M., 2010. Pathogenesis of pandemic influenza A (H1N1) and triple-reassortant swine influenza A (H1) viruses in mice. J. Virol. 84 (9), 4194–4203.

Bergmann, M., Garcia-Sastre, A., Carnero, E., Pehamberger, H., Wolff, K., Palese, P., Muster, T., 2000. Influenza virus NS1 protein counteracts PKR-mediated inhibition of replication. J. Virol. 74 (13), 6203–6206.

Boon, A.C., deBeauchamp, J., Hollmann, A., Luke, J., Kotb, M., Rowe, S., Finkelstein, D., Neale, G., Lu, L., Williams, R.W., Webby, R.J., 2009. Host genetic variation affects resistance to infection with a highly pathogenic H5N1 influenza A virus in mice. J. Virol. 83 (20), 10417–10426.

Boon, A.C., Debeauchamp, J., Krauss, S., Rubrum, A., Webb, A.D., Webster, R.G., McElhaney, J., Webby, R.J., 2010. Cross-reactive neutralizing antibodies directed against pandemic H1N1 2009 virus are protective in a highly sensitive DBA/2 influenza mouse model. J. Virol. 84 (15), 7662–7667.

Bouvier, N.M., Palese, P., 2008. The biology of influenza viruses. Vaccine 26 (Suppl. 4), D49–D53.

Budd, A., Alleva, L., Alsharifi, M., Koskinen, A., Smythe, V., Arno Mullbacher, A., Wood, J., Clark, I., 2007. Increased survival after gemfibrozil treatment of severe mouse influenza. Antimicrob. Agents Chemother. 51, 2965–2968.

Couceiro, J.N., Paulson, J.C., Baum, L.G., 1993. Influenza virus strains selectively recognize sialyloligosaccharides on human respiratory epithelium; the role of the host cell in selection of hemagglutinin receptor specificity. Virus Res. 29 (2), 155–165.

de Jong, M.D., Simmons, C.P., Thanh, T.T., Hien, V.M., Smith, G.J., Chau, T.N., Hoang, D.M., Chau, N.V., Khanh, T.H., Dong, V.C., Qui, P.T., Cam, B.V., Ha do, Q., Guan, Y., Peiris, J.S., Chinh, N.T., Hien, T.T., Farrar, J., 2006. Fatal outcome of human influenza A (H5N1) is associated with high viral load and hypercytokinemia. Nat. Med. 12 (10), 1203–1207.

Ding, M., Lu, L., Toth, L.A., 2008. Gene expression in lung and basal forebrain during influenza infection in mice. Genes Brain Behav. 7 (2), 173–183.

Ducatez, M.F., Webster, R.G., Webby, R.J., 2008. Animal influenza epidemiology. Vaccine 26 (Suppl. 4), D67–D69.

Gabriel, G., Herwig, A., Klenk, H.D., 2008. Interaction of polymerase subunit PB2 and NP with importin alpha1 is a determinant of host range of influenza A virus. PLoS Pathog. 4 (2), e11.

Gao, P., Watanabe, S., Ito, T., Goto, H., Wells, K., McGregor, M., Cooley, A.J., Kawaoka, Y., 1999. Biological heterogeneity, including systemic replication in mice, of H5N1 influenza A virus isolates from humans in Hong Kong. J. Virol. 73 (4), 3184–3189.

Gazit, R., Gruda, R., Elboim, M., Arnon, T.I., Katz, G., Achdout, H., Hanna, J., Qimron, U., Landau, G., Greenbaum, E., Zakay-Rones, Z., Porgador, A., Mandelboim, O., 2006. Lethal influenza infection in the absence of the natural killer cell receptor gene Ncr1. Nat. Immunol. 7 (5), 517–523.

Gottfredsson, M., Halldorsson, B.V., Jonsson, S., Kristjansson, M., Kristjansson, K., Kristinsson, K.G., Love, A., Blondal, T., Viboud, C., Thorvaldsson, S., Helgason, A., Gulcher, J.R., Stefansson, K., Jonsdottir, I., 2008. Lessons from the past: familial aggregation analysis of fatal pandemic influenza (Spanish flu) in Iceland in 1918. Proc. Natl Acad. Sci. USA 105 (4), 1303–1308.

Grimm, D., Staeheli, P., Hufbauer, M., Koerner, I., Martínez-Sobrido, L., Solorzano, A., García-Sastre, A., Haller, O., Kochs, G., 2007. Replication fitness determines high virulence of influenza A virus in mice carrying functional Mx1 resistance gene. PNAS 104 (16), 6806–6811.

Haller, O., Arnheiter, H., Lindenmann, J., 1976. Genetically determined resistance to infection by hepatotropic influenza A virus in mice: effect of immunosuppression. Infect. Immun. 13 (3), 844–854.

Haller, O., Staeheli, P., Kochs, G., 2009. Protective role of interferon-induced Mx GTPases against influenza viruses. Rev. Sci. Tech. 28 (1), 219–231.

Hatta, Y., Hershberger, K., Shinya, K., Proll, S.C., Dubielzig, R.R., Hatta, M., Katze, M.G., Kawaoka, Y., Suresh, M., 2010. Viral replication rate regulates clinical outcome and CD8 T cell responses during highly pathogenic H5N1 influenza virus infection in mice. PLoS Pathog. 6 (10).

Herold, S., Steinmueller, M., von Wulffen, W., Cakarova, L., Pinto, R., Pleschka, S., Mack, M., Kuziel, W.A., Corazza, N., Brunner, T., Seeger, W., Lohmeyer, J., 2008. Lung epithelial apoptosis in influenza virus pneumonia: the role of macrophage-expressed TNF-related apoptosis-inducing ligand. J. Exp. Med. 205 (13), 3065–3077.

Hoffmann, E., Krauss, S., Perez, D., Webby, R., Webster, R.G., 2002. Eight-plasmid system for rapid generation of influenza virus vaccines. Vaccine 20 (25–26), 3165–3170.

Horby, P., Sudoyo, H., Viprakasit, V., Fox, A., Thai, P.Q., Yu, H., Davila, S., Hibberd, M., Dunstan, S.J., Monteerarat, Y., Farrar, J.J., Marzuki, S., Hien, N.T., 2010. What is the evidence of a role for host genetics in susceptibility to influenza A/H5N1? Epidemiol. Infect. 1–9.

Jang, H., Boltz, D., Sturm-Ramirez, K., Shepherd, K.R., Jiao, Y., Webster, R., Smeyne, R.J., 2009. Highly pathogenic H5N1 influenza virus can enter the central nervous system and induce neuroinflammation and neurodegeneration. Proc. Natl Acad. Sci. USA. 106 (33), 14063–14068.

Kash, J.C., Tumpey, T.M., Proll, S.C., Carter, V., Perwitasari, O., Thomas, M.J., Basler, C.F., Palese, P., Taubenberger, J.K., Garcia-Sastre, A., Swayne, D.E., Katze, M.G., 2006. Genomic analysis of increased host immune and cell death responses induced by 1918 influenza virus. Nature 443 (7111), 578–581.

Koerner, I., Kochs, G., Kalinke, U., Weiss, S., Staeheli, P., 2007. Protective role of beta interferon in host defense against influenza A virus. J. Virol. 81 (4), 2025–2030.

Krug, R.M., 2006. Virology. Clues to the virulence of H5N1 viruses in humans. Science 311 (5767), 1562–1563.

La Gruta, N.L., Kedzierska, K., Stambas, J., Doherty, P.C., 2007. A question of self-preservation: immunopathology in influenza virus infection. Immunol. Cell Biol. 85 (2), 85–92.

Matrosovich, M.N., Matrosovich, T.Y., Gray, T., Roberts, N.A., Klenk, H.D., 2004. Human and avian influenza viruses target different cell types in cultures of human airway epithelium. Proc. Natl Acad. Sci. USA 101 (13), 4620–4624.

Palamara, A.T., Nencioni, L., Aquilano, K., De Chiara, G., Hernandez, L., Cozzolino, F., Ciriolo, M.R., Garaci, E., 2005. Inhibition of influenza A virus replication by resveratrol. J. Infect. Dis. 191 (10), 1719–1729.

Perrone, L.A., Plowden, J.K., Garcia-Sastre, A., Katz, J.M., Tumpey, T.M., 2008. H5N1 and 1918 pandemic influenza virus infection results in early and excessive infiltration of macrophages and neutrophils in the lungs of mice. PLoS Pathog. 4 (8), e1000115.

Pleschka, S., Wolff, T., Ehrhardt, C., Hobom, G., Planz, O., Rapp, U.R., Ludwig, S., 2001. Influenza virus propagation is impaired by inhibition of the Raf/MEK/ERK signalling cascade. Nat. Cell Biol. 3 (3), 301–305.

Rolling, T., Koerner, I., Zimmermann, P., Holz, K., Haller, O., Staeheli, P., Kochs, G., 2009. Adaptive mutations resulting in enhanced polymerase activity contribute to high virulence of influenza A virus in mice. J. Virol. 83 (13), 6673–6680.

Salomon, R., Webster, R.G., 2009. The influenza virus enigma. Cell 136 (3), 402–410.

Scheiblauer, H., Kendal, A.P., Rott, R., 1995. Pathogenicity of influenza A/Seal/Mass/1/80 virus mutants for mammalian species. Arch. Virol. 140 (2), 341–348.

Schickli, J.H., Flandorfer, A., Nakaya, T., Martinez-Sobrido, L., García-Sastre, A., Palese, P., 2001. Plasmid-only rescue of influenza A virus vaccine candidates. Philos Trans R Soc Lond B Biol Sci 356 (1416), 1965–1973.

Scriven, J., McEwen, R., Mistry, S., Green, C., Osman, H., Bailey, M., Ellis, C., 2009. Swine flu: a Birmingham experience. Clin. Med. 9 (6), 534–538.

Song, M.S., Pascua, P.N., Lee, J.H., Baek, Y.H., Lee, O.J., Kim, C.J., Kim, H., Webby, R.J., Webster, R.G., Choi, Y.K., 2009. The polymerase acidic protein gene of influenza A virus contributes to pathogenicity in a mouse model. J. Virol. 83 (23), 12325–12335.

Srivastava, B., Blazejewska, P., Hessmann, M., Bruder, D., Geffers, R., Mauel, S., Gruber, A.D., Schughart, K., 2009. Host genetic background strongly influences the response to influenza a virus infections. PLoS ONE 4 (3).

Ten Haaft, P., Verstrepen, B., Uberla, K., Rosenwirth, B., Heeney, J., 1998. A pathogenic threshold of virus load defined in simian immunodeficiency virus- or simian–human immunodeficiency virus-infected macaques. J. Virol. 72 (12), 10281–10285.

Tumpey, T.M., Garcia-Sastre, A., Taubenberger, J.K., Palese, P., Swayne, D.E., Pantin-Jackwood, M.J., Schultz-Cherry, S., Solorzano, A., Van Rooijen, N., Katz, J.M., Basler, C.F., 2005. Pathogenicity of influenza viruses with genes from the 1918 pandemic virus: functional roles of alveolar macrophages and neutrophils in limiting virus replication and mortality in mice. J. Virol. 79 (23), 14933–14944.

Tumpey, T.M., Szretter, K.J., Van Hoeven, N., Katz, J.M., Kochs, G., Haller, O., Garcia-Sastre, A., Staeheli, P., 2007. The Mx1 gene protects mice against the pandemic 1918 and highly lethal human H5N1 influenza viruses. J. Virol. 81 (19), 10818–10821.

Weis, W., Brown, J.H., Cusack, S., Paulson, J.C., Skehel, J.J., Wiley, D.C., 1988. Structure of the influenza virus haemagglutinin complexed with its receptor, sialic acid. Nature 333, 426–431.

Wurzer, W.J., Planz, O., Ehrhardt, C., Giner, M., Silberzahn, T., Pleschka, S., Ludwig, S., 2003. Caspase 3 activation is essential for efficient influenza virus propagation. EMBO J. 22 (11), 2717–2728.

Yates, L., Pierce, M., Stephens, S., Mill, A., Spark, P., Kurinczuk, J., Valappil, M., Brocklehurst, P., Thomas, S., Knight, M., 2010. Influenza A/H1N1v in pregnancy: an investigation of the characteristics and management of affected women and the relationship to pregnancy outcomes for mother and infant. Health Technol. Assess. 14 (34), 109–182.

Yen, H.L., Aldridge, J.R., Boon, A.C., Ilyushina, N.A., Salomon, R., Hulse-Post, D.J., Marjuki, H., Franks, J., Boltz, D.A., Bush, D., Lipatov, A.S., Webby, R.J., Rehg, J.E., Webster, R.G., 2009. Changes in H5N1 influenza virus hemagglutinin receptor binding domain affect systemic spread. Proc. Natl Acad. Sci. USA 106 (1), 286–291.

Zheng, B.J., Chan, K.W., Lin, Y.P., Zhao, G.Y., Chan, C., Zhang, H.J., Chen, H.L., Wong, S.S., Lau, S.K., Woo, P.C., Chan, K.H., Jin, D.Y., Yuen, K.Y., 2008. Delayed antiviral plus immunomodulator treatment still reduces mortality in mice infected by high inoculum of influenza A/H5N1 virus. Proc. Natl Acad. Sci. USA 105 (23), 8091–8096.